Genes, Brain and Behavior (2007) **6:** 30–41

Estimating wall guidance and attraction in mouse free locomotor behavior

G. Horev[*,†], Y. Benjamini[‡], A. Sakov[‡] and I. Golani[†]

[†]Department of Zoology, George S. Wise Faculty of Life Sciences, and [‡]Department of Statistics and Operations Research, The Sackler Faculty of Exact Sciences, Tel Aviv University, Tel Aviv, Israel
**Corresponding author: G. Horev, Department of Zoology, George S. Wise Faculty of Life Sciences, Tel Aviv University, Tel Aviv, Israel. E-mail: horevguy@post.tau.ac.il*

In this study, we estimate the influence exerted by the wall of the Open Field on the trajectory of the mouse. The wall exerts two types of influence on the mouse's path: one of guidance and one of attraction. The guiding influence is expressed by the tendency of mice to progress in parallel to the wall. This tendency wanes with increasing distance from the wall but is observed at large distances from it. The more parallel the mouse is to the wall the higher is its speed, even when distant from the wall. This association between heading direction and speed shows that the mouse controls its heading in reference to the wall. It is also observed in some blind strains, revealing that wall-guidance is not based exclusively on vision. The attraction influence is reflected by movement along the wall and by the asymmetry between speed during movement toward, and during movement away from the wall: sighted mice move faster toward the wall, whereas blind mice use similar speeds in both directions. Measures characterizing these influences are presented for five inbred strains, revealing heritable components that are replicable across laboratories. The revealed structure can lead to the identification of distinct groups of genes that mediate the distinct influences of guidance and attraction exerted by the wall. It can also serve as a framework for the decoding of electrophysiological data recorded in free moving rodents in the Open Field.

Keywords: Heading direction, navigation, open field, phenotyping, spatial orientation, thigmotaxis

Received 16 October 2005, revised 9 January 2006, accepted for publication 27 January 2006

Studies of exploration often use the path traced by a mouse in the open field to reveal genetic, pharmacological, or lesion effects underlying path properties (Crawley *et al*. 1997; Hall 1934, 1936). Researchers in these fields often characterize the path using cumulative measures, such as the distance traveled throughout a session, and the proportion of time spent in the center (Crawley *et al*. 1997). In contrast, studies investigating neural processes related to navigation focus on measuring moment-to-moment location (O'Keefe 1976; O'Keefe & Dostrovsky 1971), speed (King *et al*. 1998; McNaughton *et al*. 1983) and heading direction (Taube *et al*. 1990; Wiener & Taube 2005), and relate these measurements to neuron firing patterns in the CNS (e.g. Hafting *et al*. 2005; McNaughton *et al*. 1996). In both cases, the phenomenology of the momentary relations between these kinematic variables in a free-moving rodent has not been studied. The results of such study could serve as guideline in the study of neural and genetic mechanisms underlying path structure.

In this study, we measure the mouse's momentary location, heading direction and speed during Open Field behavior, describe regularities that link these three variables into patterns and show that these patterns have a heritable component replicable across three laboratories.

We track mouse movement in a 2.5-m-diameter arena, thus imposing an extended gradient between the wall and the center. The small mouse image in such a large arena prevents direct measurement of the mouse's heading. The noise generated by the tracking system and the erratic nature of mouse locomotor behavior present a challenge for a reliable estimate of the animal's speed and heading direction. To reduce noise, we use statistical smoothing algorithms to estimate locations and momentary velocities of the animal (Hen *et al*. 2004). Then we segment the smoothed path data into units of progression and units of lingering, or staying-in-place behavior (Drai & Golani 2001). Next, the lingering episodes are removed, leaving segments of uninterrupted progression. Finally, we calculate the momentary heading direction in the smoothed progression segments using the angular component of the mouse's velocity vector.

Because the wall influences the mouse's path (Crawley *et al*. 1997), we describe the mouse's location and direction of progression in a wall-related frame of reference. This frame complements the conventional Cartesian and absolute frames used in navigation-related studies (Hafting *et al*. 2005; O'Keefe & Dostrovsky 1971; Taube *et al*. 1990). Using distance from wall (distance) and heading direction in reference to the wall (heading) reveals that the wall constraints heading, and this effect wanes gradually with distance. Furthermore, heading influences speed at large

doi: 10.1111/j.1601-183X.2006.00216.x

distances from the wall. Thus, instead of the commonly used discrete distinction between movement along the wall and center occupancy, we describe a continuous gradient extending into the center. Because the wall's influence is measurable, strain-specific and replicable across laboratories, our results can be used as guideline in the analysis of genetic and neurophysiologic processes mediating the trajectory's structure.

Materials and methods

Data were collected in a study conducted simultaneously in three laboratories: The National Institute on Drug Abuse (NIDA; Baltimore, MD, USA), Maryland Psychiatric Research Center (MPRC; Baltimore, MD, USA) and Tel Aviv University (TAU; Tel Aviv, Israel). These data are stored in a publicly available database (http://www.tau.ac.il/~ilan99/see/help) and have already been used in previous studies (Kafkafi & Elmer 2005; Kafkafi *et al*. 2005; Lipkind *et al*. 2004). The study included 10 inbred mouse strains and is part of the Mouse Phenome Database (Paigen & Eppig 2000). The experimental and housing protocols are described in detail elsewhere (Kafkafi *et al*. 2003). Here, we repeat the main points.

Animals

In the present study, we selected the data of five strains that show relatively high activity in the center of the arena [C57BL/6J (C57), CZECHII/Ei (CZECHII), FVB/NJ (FVB), SJL/J (SJL) and C3H/HeJ (C3H)]. The last three strains are known to be homozygous for the retinal degeneration allele *Pde6b*^{rd1} and were either blind or visually strongly impaired by the age they were tested (Chang *et al*. 2002).

Male mice, 9- to 14-week old, were shipped from Jackson Laboratories. Animals were maintained in a 12:12 h reversed-light cycle (lights on from 2000 to 0800 h) and were housed two to four per cage under standard conditions of 22 °C room temperature and water and food *ad libitum*. The animals were housed in their room for at least 2 weeks before the start of the experiment. All animals were maintained in facilities fully accredited by the American Association for the Accreditation of Laboratory Animal Care (AAALAC, MPRC and NIDA) or by National Institutes of Health Animal Welfare Assurance Number A5010-01 (TAU). The study was conducted in accordance with the National Research Council's Guide for the Care and Use of Laboratory Animals.

Experimental procedure

The arena was a 2.5-m-diameter circular area with a nonporous gray floor and a 50-cm high primer gray-painted continuous wall. Several landmarks of various shapes and sizes were attached to different locations on the arena wall and on the walls of the room where the arena was located. The arena was illuminated with two 40 W neon bulbs on the ceiling above the center of the arena. The experiments were conducted during the dark part of the cycle 1–2 h after its onset. Each experimental animal was brought from its housing room to the arena in a small opaque box and placed within the arena (in a standardized location, near the wall) while still in the box. After 20 seconds, the box was lifted and a 30-min session began. The animal's movement was tracked with the Noldus EthoVision automated tracking system (Spink *et al*. 2001).

Data analysis

The raw data obtained from the tracking system were smoothed with the use of a specialized algorithm implemented in the stand-alone program 'SEE Path Smoother' (Hen *et al*. 2004). This procedure produces reliable estimates of momentary speeds during motion (momentary speeds during arrests were defined as zero). As was previously shown, rodent locomotor behavior consists of two distinct modes of motion: progression segments and lingering episodes (Drai *et al*. 2000; Golani *et al*. 1993). During progression segments, the animals traverse relatively large distances, attaining relatively high speeds. During lingering episodes, the animals stop and perform scanning movements, while staying in a circumscribed neighborhood. Segmentation of the smoothed path into progression segments and lingering episodes was done with the expectation maximization algorithm (e.g. Everitt 1981), using a two-Gaussian mixture model. Stand-alone user-friendly software for smoothing (SEE Path Smoother) and for segmentation (SEE Path Segmentor) can be downloaded at http://www.tau.ac.il/~ilan99/see/help.

Heading calculation

The method of calculation of heading, and the time series of heading, distance from wall and speed, derived from the data of a particular path traced by a mouse is illustrated in Fig. 1.

The heading variable measures the direction of progression of the animal in relation to the wall (and not in relation to a fixed absolute direction) during progression segments. The heading value is the angle between the direction of the animal's velocity vector and a line extending from the center of the arena to the animal's current location (Fig. 1b). When the animal moves in parallel (0°, 180°) to the wall or at right angles to it (90°, 270°), the heading values are stable (Fig. 1a,c). Heading values were transformed to values between −90° (toward the wall) and 90° (away from the wall), so that progression in parallel to the wall (0°, 180°, 360°) acquires a value of 0°.

During progression near the center (distances larger than 90 cm from wall), heading values are noisy. This is reflected in an increase in the variability of heading near the center. In the *Results* section, the arena was partitioned into three concentric rings and a central disk, starting at a distance of

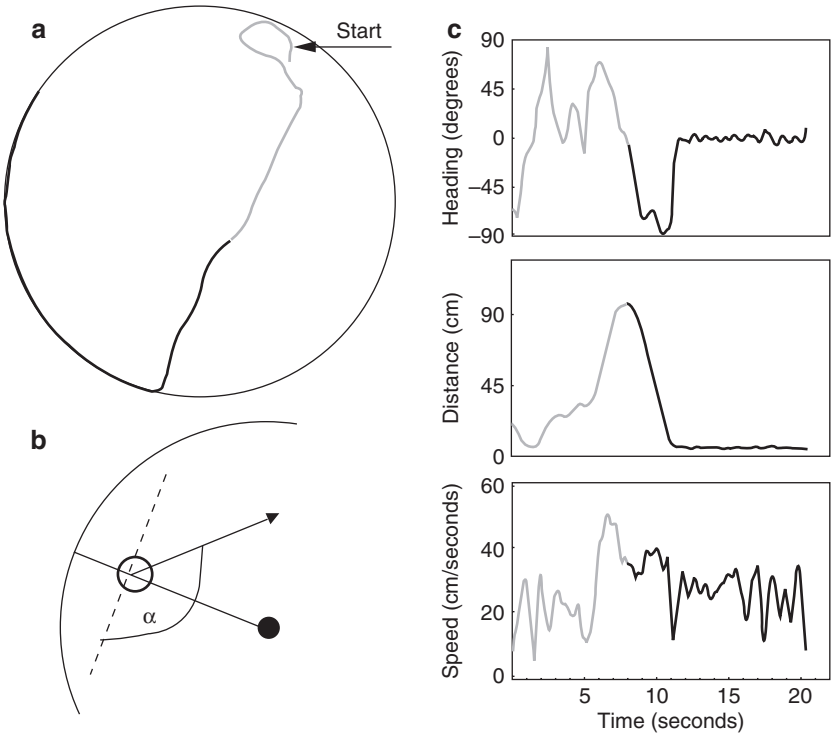

Figure 1: An illustration of the dynamics of heading direction, distance from wall and speed, during the performance of a single progression segment. (a) Path data within the circular arena. (b) The method of calculation of momentary heading direction: The large arc designates the wall of the arena, the small empty circle – the mouse's location, the small full circle – the center of the arena, and the arrow – the mouse's direction of progression. α is the angle between the mouse's direction of progression and a line perpendicular to the arena's radius. It describes the mouse's momentary heading direction. (c) The time series of the three measured variables for the path in (a). In graphs (a) and (c), gray line stands for movement until maximal distance from wall is reached, and black line stands for movement away from point of maximal distance. Note that during progression in parallel to the wall heading direction stabilizes around 0°.

37 cm from wall. Because the vast majority of the movement in this disk took place in distances smaller than 90 cm from wall, the estimation of heading variability reflects an absence of preference for a particular heading, and not center-related noise.

Relative speed calculation

To provide a common scale that will allow a comparison of speed dynamics between strains that differ greatly in their speeds, we normalize the speed data. The relative speed variable is calculated for each mouse separately by subtracting its minimal speed within all progression segments from the momentary speed at each time point and then dividing the remainders by the 95th speed quantile (which is more stable than the maximum) of all progression segments.

Mathematica®-based program SEE Package (Drai & Golani 2001) and two extension programs, 'SEE Experiment Explorer' and 'SEE End-point Manager' (Kafkafi 2003), were used to develop the new heading and relative speed measures and the behavioral measures (end-points) described in the *Results* section.

Visualization of the relations between distance heading and speed

To establish the relationship between these variables, we plotted the variables in a running window of 5% of the data points obtained for progression segments throughout the session (Figs 4, 5 and 7). The phrase 'in heading 0°' thus refers throughout the text to 'in a window of 5% of the data around heading 0°'.

Statistical methods

Comparing end-point results between strains and across laboratories

To assess the discrimination between strains and the replicability across laboratories of heading-related end-points (see *Results*), we used the linear mixed-effects ANOVA model (McCulloch & Searle 2001; Neter *et al.* 1996) with strain being considered as a fixed factor, while the effect of laboratory is considered as random and so is the interaction between strain and laboratory (Kafkafi *et al.* 2005). In this model, the yardstick for a significant strain difference includes variability across individuals, variability across laboratories and variability across the strain–laboratory interaction. The across-laboratories variability may be large, but when comparing strains across laboratories, this term is cancelled out. In contrast, the strains–laboratory interaction, which may be large too, does not cancel out. By including the interaction term in the yardstick, the mixed model thus sets a higher benchmark for showing a significant genotype difference than that used in the traditional fixed model. This approach is more conservative than the widely used linear fixed-effects ANOVA model: if a difference between two strains was found to be significant under the mixed model, it will also be significant under the fixed-effects model, but the opposite is not necessarily true. Analysis

was performed on transformed data, whose distribution is close to the normal distribution, and its variances are stabilized. From the mixed model results, the proportion of variance attributed to each factor (genotype, laboratory, their interaction and the 'residuals' or within animal) was computed (Kafkafi *et al*. 2005). Note that the proportion of genotype variance is a relatively conservative estimation of the broad sense heritability. For a detailed exposition of the use of the mixed-effects ANOVA model to assess discrimination between mouse strains and replicability across laboratories, see Kafkafi *et al*. (2005).

Pairwise comparisons

For all end-points which were found significant (using the mixed ANOVA model), assessing which strains are significantly different from each other is of interest. Therefore, all possible pairs of strains were tested for a significant difference in each end point. For that matter, a variation on the pairwise '*t*-tests' was performed. The denominator of the *t*-value (i.e. the standard error of the difference in means) was computed using all components of variance (unlike the traditional model in which there is only one variance component). The degrees of freedom were found using Satterthwaite's approximation (Littell *et al*. 1996; Satterthwaite 1946).

Correction for multiple comparisons

The false discovery rate (FDR) controlling procedure of Benjamini and Hochberg (1995) was used to control for multiple comparisons, first for the comparison of end-point results between strains and across laboratories (11 comparisons for 11 end-points) and second for the pairwise comparisons (90 comparisons for nine significant end-points $\times$ 10 pairs of strains) (Benjamini *et al*. 2001).

Results

For clarity of exposition, we first demonstrate the wall's influence on heading and speed in one strain, C57. After examining the overall frequency distribution (density) of heading throughout the arena, we study it at different distances from the wall. Next, we examine the relationship between heading and speed throughout the arena, describe this relationship for different distances from the wall and compare the effects of heading and distance on speed. We conclude the C57 section by presenting a 3-D view of the relationship between heading, distance and speed. A comparison of the same phenomena in four additional strains is performed in terms of 11 end-points. Each end-point is introduced in the *Results* section, listed in Table 1, and defined algorithmically in the on-line supplement.

Density of heading values

Figure 2 shows the density of the headings in the 12 C57 mice. The symmetrical distribution around the maximum at heading 0° (designating progression in parallel to the wall) in each of the mice allows us to characterize the distribution by estimating the inter-quartile range (IQR) of heading. The IQR provides a measure of the tendency of the mouse to deviate from the median (see 'Overall variability of heading directions' in Table 1). The wider the density plot (and therefore the lower the maximum), the higher the IQR value is. To examine whether the high density around 0° merely reflects the fact that most progression occurs near the wall, we studied the IQR of heading at four ranges of distance from the wall.

The distance-from-wall influence on heading

The IQRs of heading in the four ranges of distance (three concentric rings henceforth termed rings; the central disk amounts to half of the size of the arena) are similar in the 12 examined C57 mice. In the outermost ring of 0–5 cm from the wall, the variation in heading around the 0° median is very small (between 5° and 10° IQR; see left boxplot in Fig. 3a). In the next two rings, between 5 and 15 cm, and 15–37 cm, there is a gradual increase in heading variation around the median. Finally, in the central disk, heading IQR is about 90° around 0°, reflecting an absence of a preference for a particular heading (Fig. 3a, rightmost boxplot; see *Methods*). The gradual increase in the headings IQR up to the distance of 37 cm shows that the wall's guiding influence on heading decreases with the increase in distance. It also implies that although the tendency of the mouse to move in parallel to the wall is decreasing gradually, it is still present at relatively high distances. This tendency is quantified by the end-point 'distance from wall at which constraints on heading disappear' (Table 1). A comparison reveals that the distance's influence on heading variability (Fig. 3a) is farther reaching than its effect on relative speed variability (see *Methods*; Fig. 3b). In other words, heading variability is a more sensitive estimate of the influence of distance than speed variability.

The influence of heading on speed

In Fig. 4a, we plot relative speed as a function of heading. As shown, in all mice, the speed is highest when the mouse progresses in parallel to the wall (heading 0°), dropping from this maximum in either direction. This phenomenon is quantified by two end-points: 'median of relative speed in heading 0°', and 'normalized speed median in heading 0°' (Table 1). The first end-point provides the value of the median in a window around 0°, and the second – its relative value within the minimum–maximum range obtained in all windows. The second end-point accepts values between 0 and 1, reaching a value of 1 when the median in the window around 0° is maximal, and a value of 0 when this median is minimal.

As demonstrated, in C57, the drop in speed during movement toward the wall (negative heading values) is milder than the drop during movement away from it (positive heading values). This is most conspicuous in the lower quartile line. It means that these mice progress faster toward the wall than away from it, suggesting that the wall exerts an

Table 1: Comparisons of 11 end-points based on heading, speed, and distance from wall, in the 5 mouse strains. The numbers within the cells are strain means normalized between zero and one within each end-point (the detailed description of end-point algorithms are available in the on-line supplemental material). The *P*-values are the results of a mixed ANOVA model, based on data obtained in 3 laboratories (see methods). Within each endpoint, the gray boxes represent the results of pairwise comparisons between the strains (see methods). Gray boxes that share a common level do not differ significantly from each other after the FDR adjustment (FDR adjusted *p*-value of all ≤ 0.05). Strains, in which the gray boxes occupy more than one level, do not differ significantly from the stains in these levels

	C57	CZECHII	FVB	C3H	SJL	*P*-Value	Heritability (%)
Inbound/Outbound Speed Asymmetry	0.62	0.68	0.56	0.48	0.50	0.0001	23
Overall variability of Heading directions	0.61	0.28	0.59	0.65	0.37	0.0001	33
Distance from wall in which constraints on Heading disappear	0.80	0.72	0.73	0.60	0.54	0.0001	32
Median of Relative Speed in Heading 0°	0.32	0.35	0.33	0.54	0.60	0.0001	37
Normalized speed median in Heading 0°	0.71	0.64	0.62	0.61	0.59	0.1567	3
Variability of Relative Speed in Heading 0°	0.32	0.46	0.46	0.48	0.46	0.035	9
Normalized speed variability in Heading 0°	0.54	0.53	0.48	0.32	0.23	0.0001	9
Proportion of speed in ring 1 explained by Distance	0.40	0.44	0.56	0.48	0.63	0.037	14
Proportion of speed in ring 1 explained by Heading	0.27	0.47	0.47	0.44	0.61	0.0001	28
Proportion of speed in ring 2 explained by Distance	0.61	0.58	0.59	0.66	0.80	0.0001	20
Proportion of speed in ring 2 explained by Heading	0.53	0.74	0.46	0.38	0.38	0.0001	48

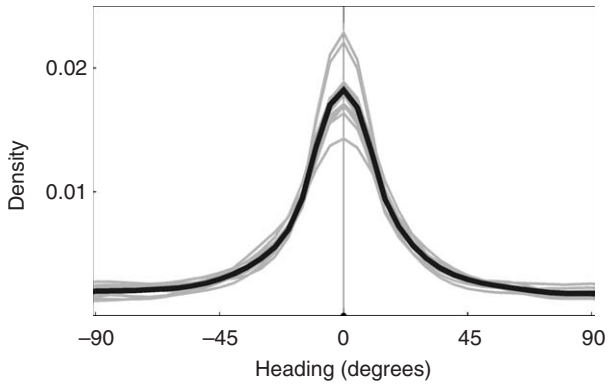

Figure 2: Density plots of heading in 12 C57 mice. The black line represents the pooled data of all mice, and the gray lines represent individual mice. As shown, each line has a maximum at heading 0°.

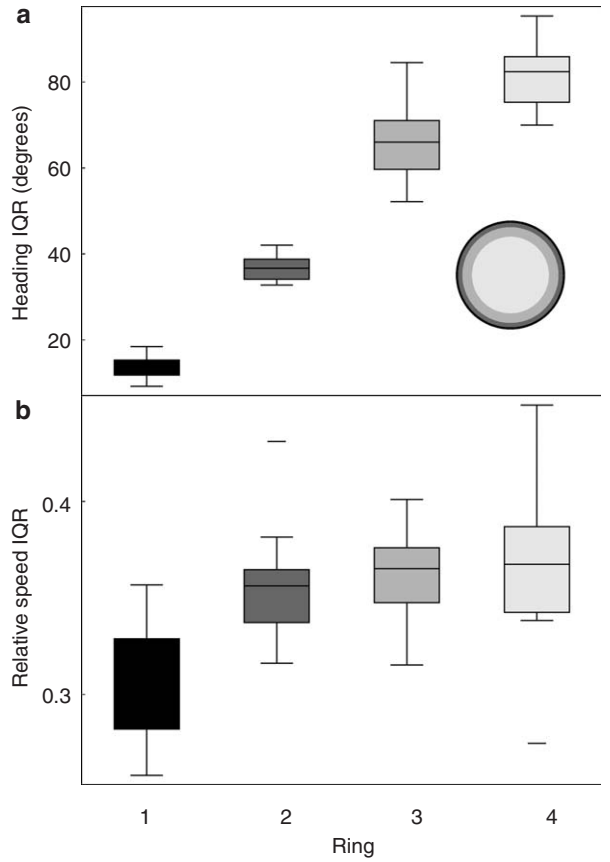

Figure 3: Ranges of heading and speed at different distances from wall. Boxplots of the interquartile range (IQR) of heading (a) and speed (b) in 12 C57 mice, in four rings, representing, from dark to bright, increasingly larger distances from wall (0–5 cm, 5–15 cm, 15–37 cm, 37–125 cm; see insert with rings in (a). Note that the increase in heading IQR extends across a long distance from wall, whereas the increase in relative speed IQR extends across a much shorter distance.

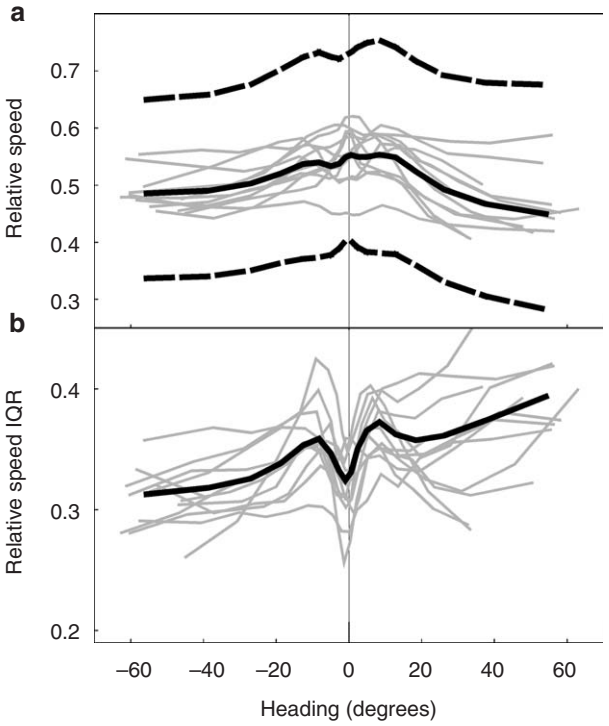

Figure 4: The influence of heading on speed. (a) medians of relative speed as a function of heading, in 12 individual C57 mice (in gray) and in the group as a whole (in black). The dashed black lines represent the lower and upper quartiles of relative speed. Note that speed is maximal in heading 0°. Also note the asymmetry between movement toward the wall (negative heading values) and movement away from wall (positive heading values), which is most conspicuous in the lower quartile. (b) Interquartile ranges (IQRs) of relative speed as a function of heading, in 12 individual C57 mice (in gray) and in the group as a whole (in black). Note that IQR is at a local minimum in heading 0°.

attraction force on the mice belonging to this strain. This phenomenon is quantified by the end-point 'inbound/outbound speed asymmetry' (Table 1).

Speed variability

To establish the degree of variability (or, for that matter, stereotypy) of speed, we examined the relationship between heading and the IQR of relative speeds (see *Methods*). A narrow IQR implies a low variability of speed. As shown in Fig. 4b, when the mice reach the highest speeds, the IQR is at a local minimum, i.e. variability is the lowest. Progressing in parallel to the wall thus constrains the variability of speeds in C57 mice, although one would expect that higher speeds would involve a wider range of exhibited speeds. This phenomenon is quantified by two end-points: 'variability of relative speed in heading 0°' and 'normalized speed variability in heading 0°' (Table 1). The first end-point provides the IQR in a window around 0°, and the second – its relative value

within the minimum–maximum range obtained in all windows. The second end-point quantifies the degree to which the IQR value is maximal (value of 1) or minimal (value of 0).

The association between heading and speed at different distance ranges from wall

Examination of speed as a function of both distance (represented by the successive rings) and heading accentuates the peaking of speed in heading 0° (Fig. 4a) and reveals additional phenomena, which could not be observed by examining speed as a function of heading alone (Fig. 4a). Figure 5a shows an association between speed and heading within rings, with a slight increase in speed across rings. In the outermost three rings, speed is maximal in heading 0°, dropping from this maximum in either direction, as the mouse progresses less parallel to the wall. The association between speed and heading disappears in the center of the arena. The gradual increase in the projection of the lines on the heading-axis expresses the corresponding gradual increase in heading variability across successively more distant rings. With increasing distance from wall, the slopes dropping from the peak become milder (see also Fig. 6).

Examination of speed as a function of distance alone (Fig. 5b) shows a slight increase in speed across rings, in particular between the first and second rings, but does not reveal an association within rings between speed and distance.

We compare the strength of the association between speed on the one hand, and heading-and-distance on the other hand, and the association between speed and distance alone, first in the same mouse-session presented in A and B (Fig. 5c), and then in 12 C57 mouse-sessions (Fig. 5d; for graphs of all 12 mice see supplemental Fig. S1). As shown, in all mice, the proportion of speed explained by heading-and-distance in the outermost three rings is always higher than that explained by distance alone. The estimates for the proportion of speed explained by distance alone, and for the proportion of speed explained by heading-and-distance, in ring 1 and in ring 2, are presented in s1.

Thus, studying speed as a function of heading-and-distance uncovers an influence exerted by the wall, from a distance, on

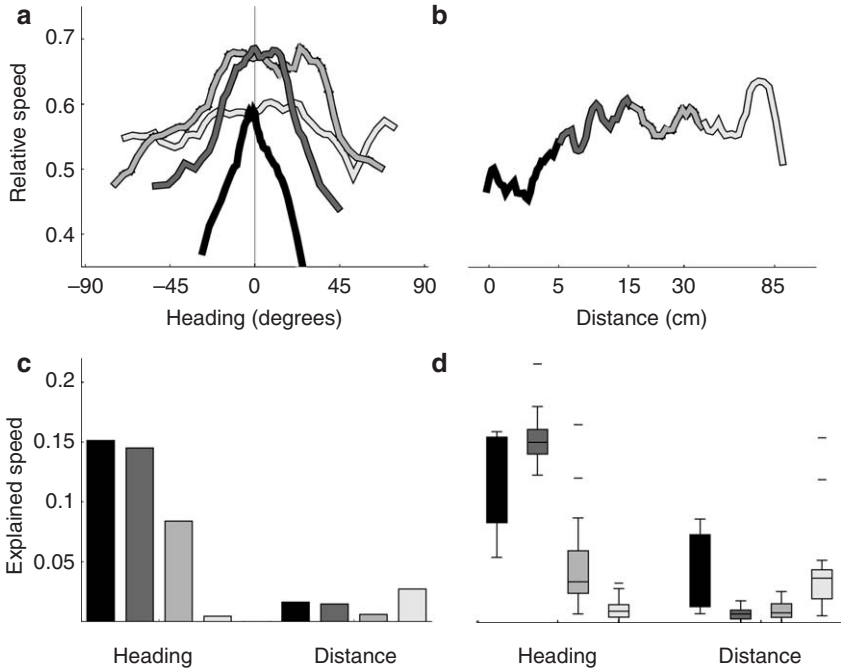

Figure 5: Speed as a function of distance alone vs. speed as a function of distance-and-heading. The gray levels of the graph lines, bars and boxes represent distance ranges from wall (0–5 cm, 5–15 cm, 15–37 cm, 37–125 cm): the brighter the color, the more distant from wall the respective ring is. (a) The medians of relative speed as a function of heading, in a single mouse session. Each graph line describes the association between heading and speed in a particular ring. Note that speed is maximal in heading 0° in the first three rings. (b) The medians of relative speed as a function of distance from wall in the same mouse-session as in (a). The absence of trend within the graph lines implies an absence of association between distance and speed within rings. (c) Estimation of the association between speed and distance alone, and the association between speed and heading-and-distance (termed heading in the graph) in the same mouse-session. Note that in the first three rings, heading explains a higher percentage of speed variation than distance. (d) Boxplots of the association values described in (c), in 12 C57 mice. The association between heading and speed gets stronger between the first and the second rings, weaker in the third ring, and disappears in the central disk. Also, in the first three rings, the association between distance and speed is weaker than that between heading and speed.

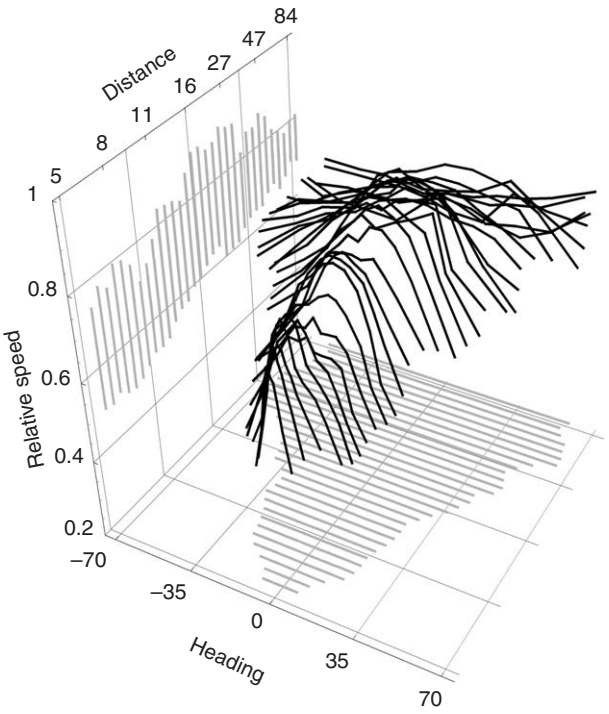

Figure 6: Relative speed plotted against heading and distance from wall in a single session of a C57 mouse. The 3-D landscape is shown in black and its projection on the distance-heading plane and the distance-speed plane is shown in gray. Medians in a running window of heading values vary between −70° and 70°. Note the slight increase in speed values depicted in the projection on the distance-speed plane, the gradual increase in heading ranges depicted in the projection on the heading-distance plane, the maximal speed in heading 0°, which forms the central ridge in the three dimensional graph, and the decrease in ridge steepness with increasing distance.

speed. This influence is averaged out by the examination of speed in relation to either heading alone or distance alone.

A 3-D landscape describing the relationship between heading, speed and distance from wall

Using a 3-D landscape plot, Fig. 6 illustrates the joint effect distance and heading exert on speed, in a specific mouse-session (for similar graphs of 12 C57, 12 FVB and 12 SJL mice, see Supplemental Figs S2, S3 and S4).

The ridge along 0° heading reflects the fact that at distances of up to about 50 cm from the wall, the speed attains a maximum in 0°. At heading smaller and greater than 0°, the speed drops steeply at small distances and increasingly more mildly at larger distances from the wall. With increasing distances, the landscape widens, encompassing a progressively wider range of heading values. The widening of the graph's projection on the heading-distance plane reflects the constraining influence the wall has on the mouse's heading. This influence wears off with distance.

Heading-related phenomena in several inbred strains

Investigation of the combined influence of heading and distance on speed in four additional inbred strains (CZECHII, FVB, SJL and C3H) reveals strain-specific values of the same features described for C57 mice. In the section below, reporting a significant difference between strains is based on a comparison of all possible pairs.

Density of heading values

In all the examined strains, as in C57, heading density reaches a maximum when the mouse progresses in parallel to the wall (Fig. 7a). CZECHII and SJL mice show a significantly higher maximum in heading 0°, whereas C57, FVB and C3H show lower amounts of movement in parallel to the wall. The IQR values (see 'overall variability of heading directions' in Table 1), which provide a measure of the tendency of a mouse to deviate from movement in heading 0°, are the lowest in CZECHII and SJL, rendering them more 'wall-guided' than the other three strains.

The distance-from-wall influence on heading

The gradual increase in heading variability (IQR) across the concentric rings (plotted only for C57 in Fig. 3a) is repeated in all the examined strains: all strains show small heading variation near the wall, followed by an increase in heading variation with increasing distance. The difference between the strains lies mainly in the rate of increase of the heading IQR. This property is captured by the end-point 'distance from wall in which constraints on heading disappear' (Table 1). C3H and SJL show the highest value of this end-point, thus indicating that in these strains the effect of the wall on heading fades rapidly. FVB, CZECHII and C57 are more constrained by the wall, with C57 being constrained to the largest distance.

The influence of heading on speed

A strain comparison of relative speed highlights the influence heading has on speed dynamics (Fig. 7b). In all the strains, speed is maximal in heading 0°. In the slow SJL, these maxima are significantly higher than in the faster strains ('median of relative speed in heading 0°', Table 1).

Examination of speed asymmetry across quartiles reveals that in the first quartile C57 and CZECHII show an asymmetry, whereas FVB, C3H and SJL do not ('inbound/outbound speed asymmetry', Table 1). This difference provides a distinction between the sighted and the blind strains. While the sighted strains exhibit an attraction to the wall, the presumably blind strains, known to be homozygous for the retinal degeneration allele *Pde6b*^{rd1} (see *Methods*) do not exhibit such attraction.

Speed variability

To compare the degree of variability of speed, we examined the IQR of relative speeds across strains (Fig. 7c). In all the strains, the values of this measure converge to a similar value in heading 0°: decrease of IQR in the fast CZECHII, C57 and FVB, while increase of IQR is evident in the slow

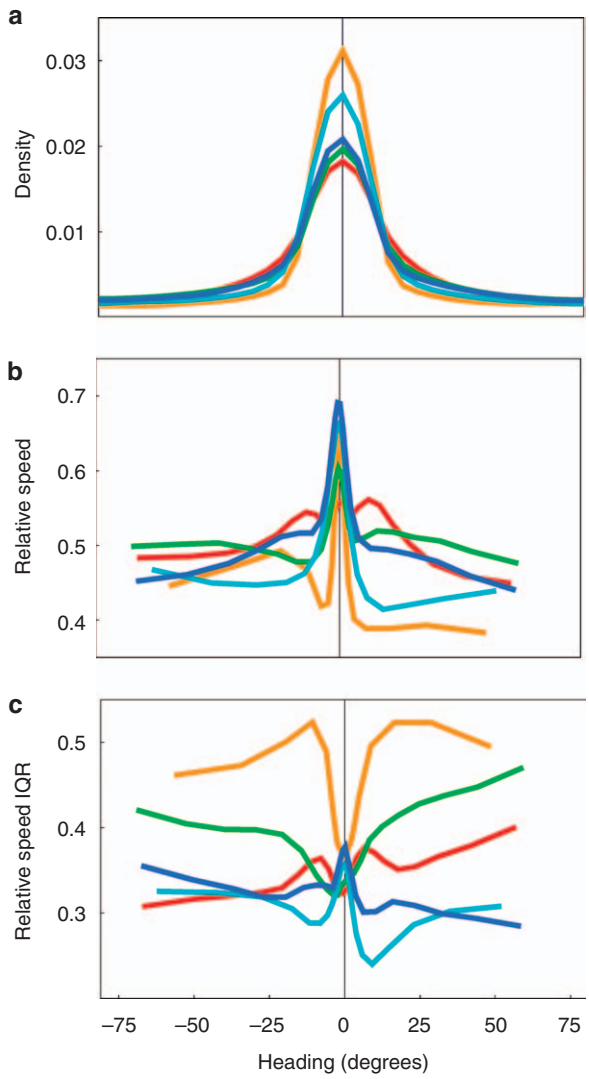

Figure 7: A strain comparison of selected heading-related phenomena. (a) Density plot of heading directions in five strains. Each strain shows a different level of preference for progression in parallel to the wall; yet, all prefer to progress in parallel to it. (b) Median and (c) inter quartile range of relative speed as a function of heading, in a running window, in five inbred mouse strains. C57 – red, CZECHII – orange, FVB – green, SJL – sky blue, C3H – dark blue. Note that in C57, CZECH and FVB, the speed is maximal in heading 0°, while interquartile range (IQR) is at a local minimum in this heading. In contrast, in C3H and SJL, both the IQR and speed are maximal in 0°. Interestingly, the IQR levels in all the strains converge to a similar value in heading 0°.

SJL and C3H strains. Because speed increases in all strains and IQR decreases in some and increases in others, increasing speed does not explain the respective changes in speed variability. In summary, progressing in parallel to the wall constrains the variability of speeds in the fast strains and expands it in the slow strains.

The association between heading and speed at different distance ranges from wall

The association between heading, distance and speed, observed in the C57 mice, is also observed in the CZECHII and FVB mice, but not in the C3H and SJL strains ('proportion of speed in ring 2 explained by heading', Table 1). This difference within the blind or visually strongly impaired group of strains suggests that vision is not the only factor mediating guidance by the wall from a distance.

A strain comparison of the heading-related end-points

Comparisons of 11 end-points based on heading, speed and distance from wall in the five mouse strains revealed significant genotype differences in nine of the 11 end-points (Table 1). Replicability of results obtained in three laboratories was tested using the mixed linear model ANOVA (Kafkafi *et al.* 2005). First, each end-point was tested to distinguish between the strains. Next, mixed ANOVA pairwise comparisons were performed on the end-points that were found to be significant in the first stage (see *Methods*). The differences remained significant even after correcting for multiple comparisons using an FDR adjustment for all possible pairs (FDR-adjusted *P*-value of all = 0.005). Taking into account the various sources of variance, we calculated the proportion of variance attributed to the genotype, which is a relatively conservative estimator of the broad-sense heritability, and found that in seven of 11 traits heritability was higher than 20%.

Discussion

In this study, we estimate the dynamics of the mouse's trajectory in a wall-related frame. In an empty arena, the wall is a boundary, a potential shelter and a most conspicuous object; therefore, the distance from it has been traditionally taken into account, revealing differences between behavior near the wall and in the center (Crawley *et al.* 1997). Distance from wall has been shown to influence neuronal activity in the rat hippocampus and related structures during a navigation-related task (O'Keefe *et al.* 1998). Heading direction has been shown to operate in reference to an absolute frame (Taube *et al.* 1990), but has not been examined in a wall-related frame. The structure of the spatial map, recently discovered by Hafting *et al.* (2005), has also been shown to be indifferent to the wall of the arena. Here, we use a complementary wall-related frame, by examining the relationship between distance from wall, speed and heading in reference to the wall. We use a large arena to establish a polarity between the area near the wall and the exposed area distant from it. Our results show that the wall exerts two types of influence on the mouse's trajectory: one of guidance and the other of attraction.

The guiding and attraction influences exerted by the wall

The guiding influence is reflected by the fact that the mice tend to progress in parallel to the wall (Figs 2 and 7a). This tendency wanes with increasing distance from wall (Fig. 3a) but is nevertheless observed in some mice at distances as far as 50 cm from the wall. Two measures express the guiding effect exerted by the wall: the overall variability of heading directions and the distance from wall in which constraints on heading disappear. Strain-specific values of these measures are presented in Table 1.

The attraction influence is reflected by the fact that mice tend to perform a large component of their activity near the wall (thigmotaxis, wall-hugging; Crawley *et al*. 1997; Lipkind *et al*. 2004). One aspect of thigmotaxis has been estimated in SEE by measuring the thickness of the ring occupied by the mouse during successive runs near the wall and in parallel to it (Lipkind *et al*. 2004). Another aspect of thigmotaxis, the proportion of progression near the wall, can be inferred from the second and third measures in Table 1. For example, because most of the SJL mice movement is performed in parallel to the wall (low overall variability of heading directions, Fig. 7a, Table 1), and because they hardly move in parallel to the wall when away from it (distance from wall in which constraints on heading disappear, Table 1), it follows that most of their progression is performed near the wall and in parallel to it.

Another measure of the degree of wall-attraction is the asymmetry between speed during movement toward, and during movement away from, the wall. The higher the speed toward the wall compared with the speed away from it, the more attracted the mouse is to the wall. This is the measure distinguishing between the blind strains, which move in similar speeds in both directions, and the sighted strains, which move faster toward the wall. The speed ratio is presented by the end-point outbound/inbound speed asymmetry in Table 1.

Different combinations of the guiding and attraction influences generate versatile strain-specific behaviors. C57 and FVB are 'guided' by the wall at large distances from it; these strains show the highest values of 'distance from wall in which constraints on heading disappear' (Table 1). These two strains are not wall-huggers; they show high heading variability (Table 1), a thick ring of paths along wall (Lipkind *et al*. 2004) and a high proportion of time spent in the center (Center Time or CNTRT in Kafkafi *et al*. 2005). In addition, C57 mice, unlike FVB mice, are attracted to the wall from a distance (higher outbound speed). CZECHII mice are guided at large distances from the wall (high value of 'distance from wall in which constraints on heading disappear'), are wall-huggers (low heading variability, most activity along wall in a thin ring of paths, low Center Time) and are strongly attracted to the wall (higher outbound speed). C3H are not wall-huggers (high heading variability and high Center Time but with relatively high variability), show no attraction to wall (no difference between outbound and inbound speeds) and no guidance at large distances from it (low value of 'distance from wall in which constraints on heading disappear'). SJL is the farthest from C57, being a wall-hugger (low heading variability, thin ring along wall and low Center Time), guided by the wall only at short distances from it (lowest value of 'distance from wall in which constraints on heading disappear') and not attracted to the wall at a distance from it (no difference between inbound and outbound speed).

These results show that the guidance and attraction measures add information to the traditional Center Time measure. This is further demonstrated in Fig. 8a,b, which shows that guidance and attraction are not correlated with Center Time. A comparison of Center Time in our arena and in smaller arenas used in other studies show a correspondence in FVB, C57 and C3H, but not in SJL (Bothe *et al*. 2004; 2005; Kim *et al*. 2002; Rogers *et al*. 1999).

Because the wall is also a boundary, it could be of interest to examine the influence of other types of boundary on the mouse's trajectory. In studies performed in our lab (A. Dvorkin, MSc thesis, and G. Horev, unpublished results), a cliff boundary caused severe problems in data acquisition because it elicited jumping off the arena in the CZECHII strain, falling off the cliff in the FVB, C3H and SJL strains, and both falling and jumping in the C57 and BALB/c strains.

Using the relationship between heading and speed to estimate guidance

Heading influences both the magnitude and the stereotypy of speed. The magnitude of speed is highest in heading 0° (Figs 5, 6 and 7b), dropping gradually as the mouse shifts away from this heading. This pertains to movement near the wall, and in some strains (C57, CZECHII, FVB), to movement at a distance from it ('proportion of speed in ring 2 explained by heading', Table 1). The use of heading and distance together as explanatory variables for the magnitude of speed discloses the influence the wall exerts from a distance on the speed of the mouse. The observation that a mouse increases its speed during progression in parallel to the wall when distant from it reveals that the mouse is guided by the wall even when not in physical contact with it. It implies that the mouse 'knows' its direction relative to the wall. This regularity in the relationship between heading and speed suggests that heading in reference to the wall is a key variable whose measurement is necessary for the understanding of open-field behavior.

The guiding effect of the wall is also indicated by the association between movement in parallel to the wall and a distinct change in the variability of speed. In each of the examined strains, movement in parallel to the wall involves a distinct variability value of speeds. In heading 0°, the speed variability reaches a maximum in the slow strains (SJL, C3H) and a minimum in the fast strains (C57, CZECHII, FVB; Fig. 7c). The maxima and minima cluster around a similar value and are indistinguishable from each other (normalized speed variability in heading 0°, Table 1).

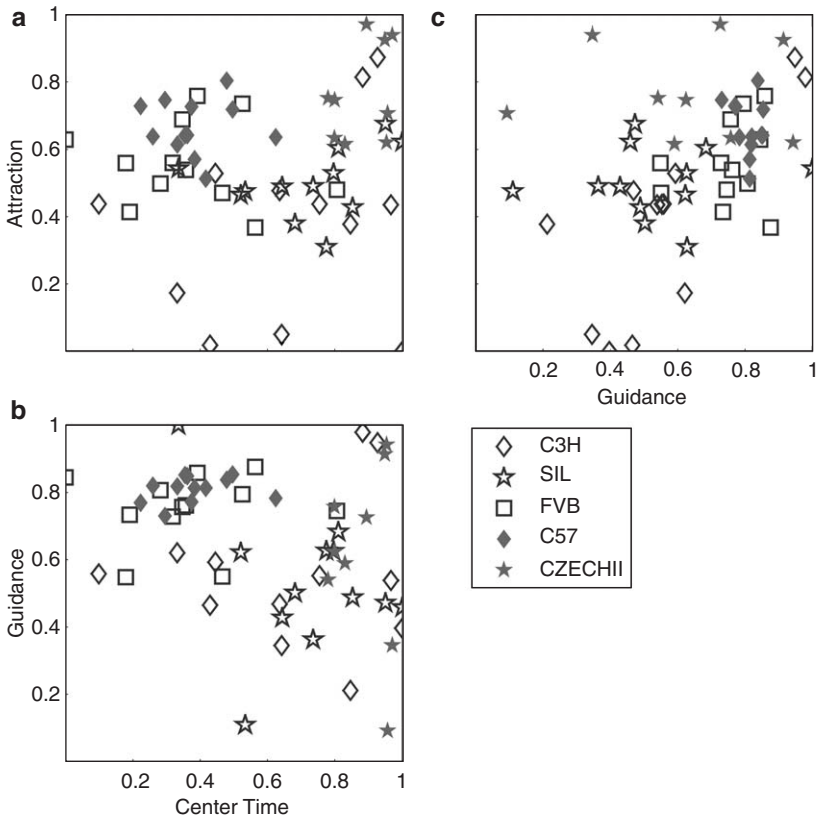

Figure 8: A pairwise scatter plot of Guidance, Attraction and Center Time. (a) Center Time vs. Attraction ('inbound/outbound speed asymmetry'); (b) Center Time vs. Guidance ('distance from wall in which constraints on heading disappear'); and (c) Guidance vs. Attraction. Strains with severe visual impairment are represented by the empty shapes and sighted strains by full shapes. Note that both guidance and attraction are independent of Center Time (and therefore provide additional information). Also note that guidance and attraction are relatively independent of each other (implying that they are mediated by different mechanisms).

Genetic aspects of wall guidance and attraction

Our results imply that the guidance and attraction influences are mediated by different mechanisms and should eventually reveal different genes:

1. By definition, two end-points, 'distance from wall in which constraints on heading disappear' ('guidance' in Fig. 8) and 'proportion of speed in ring 2 explained by heading', reflect pure components of guidance, and 1 end-point, 'inbound/outbound speed asymmetry' ('attraction' in Fig. 8), reflects a pure component of attraction. As shown in Fig. 8c and Supplemental Fig. S5, these three components are indeed not correlated.
2. The two influences vary relatively independently across strains, engendering a variety of combinations. As summarized in Table 1, each of the nine end-points classifies the examined strains into at least two groups (for example, the second end-point classifies the mice into wall-huggers and non-wall-huggers), yielding seven different classifications. It means that these nine end-points characterize relatively independent aspects of wall guidance and attraction behavior. As such, these end-points are suitable for studies aimed at the identification of genes that mediate them.

Following the high benchmark test of mixed ANOVA (Kafkafi *et al.* 2005) and the FDR test for multiple comparisons (Benjamini & Hochberg 1995; Benjamini *et al.* 2001), nine of 11 carefully designed heading-related end-points discriminate significantly between strains and are replicable across laboratories (see *Methods*). The most attractive end-point of the nine is the one estimating the influence exerted by the wall from a distance on speed ('proportion of speed in ring 2 explained by heading'), whose heritability is the highest, amounting to 48%.

In conclusion, having shown that wall guidance and attraction reflect independent and heritable mechanisms, geneticists can now locate and subsequently manipulate gene loci that mediate these relations, and students of navigation are provided with new measures of the effect these genes might have on firing patterns measured in place-, head direction- and speed-related cells.

References

Benjamini, Y. & Hochberg, Y. (1995) Controlling the false discovery rate: a practical and powerful approach to multiple testing. *J R Stat Soc Ser B-Stat Methodol* **57**, 289–300.

Benjamini, Y., Drai, D., Elmer, G., Kafkafi, N. & Golani, I. (2001) Controlling the false discovery rate in behavior genetics research. *Behav Brain Res* **125**, 279–284.

Bothe, G.W.M., Bolivar, V.J., Vedder, M.J. & Geistfeld, J.G. (2004) Genetic and behavioral differences among five inbred mouse strains commonly used in the production of transgenic and knockout mice. *Genes Brain Behav* **3**, 149–157.

Bothe, G.W.M., Bolivar, V.J., Vedder, M.J. & Geistfeld, J.G. (2005) Behavioral differences among fourteen inbred mouse strains commonly used as disease models. *Comp Med* **55**, 326–334.

Chang, B., Hawes, N.L., Hurd, R.E., Davisson, M.T., Nusinowitz, S. & Heckenlively, J.R. (2002) Retinal degeneration mutants in the mouse. *Vision Res* **42**, 517–525.

Crawley, J.N., Belknap, J.K., Collins, A., Crabbe, J.C., Frankel, W., Henderson, N., Hitzemann, R.J., Maxson, S.C., Miner, L.L., Silva, A.J., Wehner, J.M., Wynshaw-Boris, A. & Paylor & R. (1997) Behavioral phenotypes of inbred mouse strains: implications and recommendations for molecular studies. *Psychopharmacology (Berl)* **132**, 107–124.

Drai, D. & Golani, I. (2001) SEE: a tool for the visualization and analysis of rodent exploratory behavior. *Neurosci Biobehav Rev* **25**, 409–426.

Drai, D., Benjamini, Y. & Golani, I. (2000) Statistical discrimination of natural modes of motion in rat exploratory behavior. *J Neurosci Methods* **96**, 119–131.

Everitt, B.S. (1981) *Finite Mixture Distributions*. London: Chapman & Hall.

Golani, I., Benjamini, Y. & Eilam, D. (1993) Stopping behavior: constraints on exploration in rats (Rattus norvegicus) *Behav Brain Res* **53**, 21–33.

Hafting, T., Fyhn, M., Molden, S., Moser, M.B. & Moser, E.I. (2005) Microstructure of a spatial map in the entorhinal cortex. *Nature* **436**, 801–806.

Hall, C.S. (1934) Emotional behavior in the rat. I. Defecation and urination as measures of individual differences in emotionality. *J Comp Psychol* **18**, 385–403.

Hall, C.S. (1936) Emotional behavior in the rat. III. The relationship between emotionality and ambulatory activity. *J Comp Psychol* **22**, 345–352.

Hen, I., Sakov, A., Kafkafi, N., Golani, I. & Benjamini, Y. (2004) The dynamics of spatial behavior: how can robust smoothing techniques help?. *J Neurosci Methods* **133**, 161–172.

Kafkafi, N. (2003) Extending SEE for large-scale phenotyping of mouse open-field behavior. *Behav Res Methods Instrum Comput* **35**, 294–301.

Kafkafi, N. & Elmer, G.I. (2005) Activity density in the open field: a measure for differentiating the effect of psychostimulants. *Pharmacol Biochem Behav* **80**, 239–249.

Kafkafi, N., Lipkind, D., Benjamini, Y., Mayo, C.L., Elmer, G.I. & Golani, I. (2003) SEE locomotor behavior test discriminates C57BL/6J and DBA/2J mouse inbred strains across laboratories and protocol conditions. *Behav Neurosci* **117**, 464–477.

Kafkafi, N., Benjamini, Y., Sakov, A., Elmer, G.I. & Golani, I. (2005) Genotype–environment interactions in mouse behavior: a way out of the problem. *Proc Natl Acad Sci* **102**, 4619–4624.

Kim, S., Lee, S., Ryu, S., Suk, J. & Park, C. (2002) Comparative analysis of the anxiety-related behaviors in four inbred mice. *Behav Process* **60**, 181–190.

King, C., Recce, M. & O'Keefe, J. (1998) The rhythmicity of cells of the medial septum/diagonal band of Broca in the awake freely moving rat: relationships with behaviour and hippocampal theta. *Eur J Neurosci* **10**, 464–477.

Lipkind, D., Sakov, A., Kafkafi, N., Elmer, G.I., Benjamini, Y. & Golani, I. (2004) New replicable anxiety-related measures of wall vs. center behavior of mice in the open field. *J Appl Physiol* **97**, 347–359.

Littell, R.C., Milliken, G.A., Stroup, W.W. & Wolfinger, R.D. (1996) *SAS Systems for Mixed Models*. Cary, NC: SAS Publishing.

McCulloch, C. & Searle, S. (2001) *Generalized, Linear and Mixed Models*. New York: John Wiley & Sons.

McNaughton, B.L., Barnes, C.A. & O'Keefe, J. (1983) The contributions of position, direction, and velocity to single unit activity in the hippocampus of freely-moving rats. *Exp Brain Res* **52**, 41–49.

McNaughton, B.L., Barnes, C.A., Gerrard, J.L., Gothard, K., Jung, N.W., Knierim, J.J., Kudrimoti, H., Qin, Y., Skaggs, W.E., Suster, M. & Weaver, K.L. (1996) Deciphering the hippocampal polyglot: the hippocampus as a path integration system. *J Exp Biol* **199**, 173–185.

Neter, J., Kutner, M., Nachtsheim & C. & Wasserman, W. (1996) *Applied Linear Statistical Models*. Chicago, IL: Irwin.

O'Keefe, J. (1976) Place units in the hippocampus of the freely-moving rat. *Exp Neurol* **51**, 78–109.

O'Keefe, J. & Dostrovsky, J. (1971) The hippocampus as a spatial map. Preliminary evidence from unit activity in the freely-moving rat. *Brain Res* **34**, 171–175.

O'Keefe, J., Burgess, N., Donnett, J.G. & Maguire, E.A. (1998) Place cells, navigational accuracy, and the human hippocampus. *Philos Trans R Soc B* **353**, 1333–1340.

Paigen, K. & Eppig, J.T. (2000) A mouse phenome project. *Mamm Genome* **11**, 715–717.

Rogers, D.C., Jones, D.N.C., Nelson, P.R., Jones, C.M., Quilter, C.A., Robinson, T.L. & Hagan, J.J. (1999) Use of SHIRPA and discriminant analysis to characterise marked differences in the behavioural phenotype of six inbred mouse strains. *Behav Brain Res* **105**, 207–217.

Satterthwaite, F.E. (1946) An approximate distribution of estimates of variance components. *Biometrics Bull* **2**, 110–114.

Spink, A.J., Tegelenbosch, R.A., Buma, M.O. & Noldus, L.P. (2001) The EthoVision video tracking system—a tool for behavioral phenotyping of transgenic mice. *Physiol Behav* **73**, 731–744.

Taube, J.S., Muller, R.U. & Ranck, J.B. Jr (1990) Head-direction cells recorded from the postsubiculum in freely moving rats. II. Effects of environmental manipulations. *J Neurosci* **10**, 436–447.

Wiener, S.I. & Taube, J.S. (2005) *Head Direction Cells and the Neural Mechanisms of Spatial Orientation*. Cambridge, MA: MIT Press.

Acknowledgments

This study is part of the project 'Phenotyping mouse exploratory behavior' supported by NIH grant R01 NS40234. We thank Noldus Inc. for the loan of their EthoVision tracking system to Tel Aviv University. Generous funds from AstraZeneca were used to defray the cost of mice through the Mouse Phenome Project Collaborations Program. Data were submitted to the Mouse Phenome Database, a community repository for strain characteristics data and protocols. The SEE software is available from the authors at http://www.tau.ac.il/~ilan99/see/help.

Supplementary material

The following supplementary material is available for this article online: **Appendix & Figures.** Detailed description of end-points plus five associated figures.This material is available as part of the online article from http://www.blackwell-synergy.com